Biochimica et Biophysica Acta 1822 (2012) 831–842

Contents lists available at SciVerse ScienceDirect

Biochimica et Biophysica Acta

journal homepage: www.elsevier.com/locate/bbadis

Brain IL-6 elevation causes neuronal circuitry imbalances and mediates autism-like behaviors

Hongen Wei [a,e], Kathryn K. Chadman [c], Daniel P. McCloskey [d], Ashfaq M. Sheikh [a], Mazhar Malik [a], W. Ted Brown [b], Xiaohong Li [a,*]

[a] Department of Neurochemistry, NY State Institute for Basic Research in Developmental Disabilities, New York, NY 10314, USA
[b] Department of Human Genetics, NY State Institute for Basic Research in Developmental Disabilities, New York, NY 10314, USA
[c] Department of Developmental Neurobiology, NY State Institute for Basic Research in Developmental Disabilities, New York, NY 10314, USA
[d] Department of Psychology and Center for Developmental Neuroscience, College of Staten Island, New York, NY 10314, USA
[e] Shanghai Mental Health Center, Shanghai Jiao Tong University School of Medicine, Shanghai 200030, China

ARTICLE INFO

Article history:
Received 13 October 2011
Received in revised form 28 December 2011
Accepted 26 January 2012
Available online 2 February 2012

Keywords:
Autism
Cytokine
IL-6
Synapse development
Synaptic transmission
Autistic-like behavior

ABSTRACT

Abnormal immune responses have been reported to be associated with autism. A number of studies showed that cytokines were increased in the blood, brain, and cerebrospinal fluid of autistic subjects. Elevated IL-6 in autistic brain has been a consistent finding. However, the mechanisms by which IL-6 may be involved in the pathogenesis of autism are not well understood. Here we show that mice with elevated IL-6 in the brain display many autistic features, including impaired cognitive abilities, deficits in learning, abnormal anxiety traits and habituations, as well as decreased social interactions. IL-6 elevation caused alterations in excitatory and inhibitory synaptic formations and disrupted the balance of excitatory/inhibitory synaptic transmissions. IL-6 elevation also resulted in an abnormal change in the shape, length and distributing pattern of dendritic spines. These findings suggest that IL-6 elevation in the brain could mediate autistic-like behaviors, possibly through the imbalances of neural circuitry and impairments of synaptic plasticity.

Published by Elsevier B.V.

1. Introduction

Autism is a severe neurodevelopmental disorder characterized by impairments in social interaction, deficits in verbal and non-verbal communication, and repetitive behavior and restricted interests. Susceptibility to autism has been suggested to be attributable to genetic factors and environmental risk factors [1–5], but the etiology of the disorder is poorly understood. Immune aberrations consistent with a dysregulated immune response have been reported in autistic children [6]. A number of recent studies have demonstrated that various inflammatory cytokines were elevated in blood mononuclear cells, serum, plasma and cerebrospinal fluid of autistic subjects [7-13]. Vargas et al. [14] showed that IL-6, transforming growth factor (TGF)-β1 and macrophage chemoattractant protein (MCP)-1 were increased in autistic brains. Recently, our laboratory detected that levels of IL-6, IL-8, TNFα, IFNγ and GM-CSF were significantly increased in the fontal cortex of autistic subjects [15].

Recent evidence points to a crucial role for IL-6 within the central nervous system (CNS) [16,17]. IL-6 has been shown to stimulate the differentiation of astrocytes, primary dorsal root ganglion neurons, hippocampal neurons and Schwann cells [18–21]. IL-6 can be neurotoxic and may mediate associations between maternal infection and neurodevelopmental damage [22]. Samuelsson et al. [23] demonstrated that prenatal exposure to IL-6 is critical for CNS function, but may play a role in the origin of neuro-developmental and neurodegenerative diseases. Depending on the concentration, brain region and cell type, IL-6 has been shown to promote neural growth as well as to cause neuronal death [24], to protect against excitotoxicity in cortical and cerebellar neurons, as well as to enhance NMDA-induced excitotoxicity in cerebellar granule neurons [24-27]. Recently, IL-6 has also been demonstrated to promote neuronal differentiation of neural progenitor cells in the adult hippocampus [19]. Another group has elucidated a critical finding that supports the role of IL-6 in the pathogenesis of schizophrenia and autism in the context of maternal immune activation [28].

Although elevation of IL-6 is a repeated finding in autism, the exact mechanism by which an IL-6 increase may contribute to the pathogenesis of autism remains undefined. In this study, by employing an adenoviral gene delivery approach we developed a mouse model that over-expresses IL-6 in the brain, we showed for the first time that elevation of IL-6 in the mouse brain produced certain autistic features, including impaired cognitive abilities, deficits in learning, abnormal anxiety-like traits and habituation, as well as decreased

* Correspondent author at: Department of Neurochemistry, NY State Institute for Basic Research in Developmental Disabilities, 1050 Forest Hill Road, Staten Island, New York, NY 10314, USA. Tel.: +1 718 494 5265; fax: +1 718 494 2768.
E-mail addresses: xiaohongli99@gmail.com, xiaohong.li@opwdd.ny.gov (X. Li).

0925-4439/$ – see front matter. Published by Elsevier B.V.
doi:10.1016/j.bbadis.2012.01.011

social interactions in older mice. To investigate how IL-6 elevation leads to the development of autistic phenotype, we detected that an IL-6 elevation resulted in increased excitatory synaptic formations and a decreased number of inhibitory synapses. IL-6 elevation produced an increase in the length of dendritic spines and also stimulated the formation of mushroom-shaped dendritic spines. In addition, we demonstrated that IL-6 elevation reduced postexcitatory inhibition in the mouse hippocampus.

2. Materials and methods

2.1. Intraventricular injection

Mouse GFP adenovirus (Ad-GFP) and mouse GFP-IL-6 adenovirus (Ad-GFP-IL-6) were generated by Welgen (Worcester, MA). Normal C57BL/6J mice were purchased from Jackson Laboratory (Bar Harbor, Maine) and maintained in our breeding colony. On the day of birth, designated as P0.5, pups were individually anesthetized on ice, and 2 μl of Ad-GFP-IL-6 or Ad-GFP (2×10^9 genomic equivalents) was injected into each lateral ventricle using a 10-μL Hamilton syringe with a 30-gauge needle. All treatment of mice were approved by, and carried out according to the guidelines of, the Institutional Animal Care and Use Committee.

2.2. Behavioral assays

Behavioral experiments were conducted in dedicated behavioral testing rooms during the standard light phase, as previously described [29,30]. Mice were brought to a holding room in the hallway of the testing area at least 1 h prior to the start of the behavioral test. Order of testing was as follows (1) general health at age 4–6 weeks, (2) elevated plus-maze at age 4–5 weeks, (3) social approach at age 18 weeks, (4) fear conditioning at age 6–7 weeks, (5) rotarod at age 7 weeks, (6) open field test at age 7–8 weeks, and (7) Morris water maze at age 7–8 weeks. The same cohort of animals including both females and males were used for all behavioral studies. The n values refer to the number of animals analyzed for each treatment group. *General health, neurological reflexes, sensory and motor abilities.* The general health of the mice was evaluated at age 4–5 weeks. Briefly, empty cage behavior was scored by placing the mouse into a clean, empty cage and noting incidents of transfer freezing, wild running, stereotypies, and grooming and exploration levels. General health assessment included assessing body weight, fur and whisker condition, limb and body tone. Neurological reflex tests included forepaw reaching, righting reflex, trunk curl, whisker twitch, ear twitch, and corneal reflex. The reactivity level of the mice was assessed with tests measuring responsiveness to petting, intensity of dowel biting response and level of vocalization during handling. *Elevated plus-maze*. The elevated (95 cm) plus maze consists of 2 open arms (30×5 cm) and 2 closed arms ($30\times5\times15$ cm) extending from a central (5×5 cm) area. A raised lip (0.25 cm) around the open arms minimized falling off the edges of the open arms. Mice were placed in the central area facing an open arm and allowed to traverse the maze freely for 5 min. Arm entries (70% of mouse in the arm) and time spent in the open and closed arms were tracked and scored using ANYmaze software (Stoelting, Inc., Wood Dale, IL). The center of the maze was lighted to 26 lx with 2 desk lamps angled away from the maze. *Sociability.* This experiment has two habituation phases (center and all 3 chambers) followed by the sociability testing phases. The test compares the preference for a social stimulus versus an inanimate object. Social approach behaviors were tested in an apparatus with 3 chambers in a single 30-min session, divided into 3 phases. The subject mouse was acclimated to the apparatus for 10 min in the center chamber (phase 1), and then for an additional 10 min with access to all 3 empty chambers (phase 2). The subject was then confined to the middle chamber, while the novel object (an inverted wire cup, Galaxy Cup, Kitchen Plus, Streetsboro, OH) was placed into one of the side chambers, and the stranger mouse, inside an identical inverted wire cup, was placed in the opposite side chamber. The C57BL/6J mice, aged 9–11 weeks old were used as the stranger mice. The location (left or right) of the novel object and stranger mouse alternated across subjects. The chamber doors were opened simultaneously, and the subject had access to all 3 chambers for 10 min (phase 3). Video tracking with ANYmaze automatically scored the time spent in each of the 3 chambers, time spent sniffing, and number of entries into each chamber during each 10-min phase of the test. Animals used as strangers were C57BL/6J mice habituated to the testing chamber for 30-min sessions on 3 consecutive days and were enclosed in the wire cup to ensure that all social approach was initiated by the subject mouse. An upright plastic drinking cup weighed down with a lead weight was placed on top of each of the inverted wire cups to prevent the subject mouse from climbing on top. Both end chambers maintained a lighting level of 26–27 lx with 2 desk lamps angled away from the maze. *Contextual and cued fear conditioning.* Standard trace fear conditioning was conducted. Mice were trained and scored for freezing behavior to the same environmental context in a clear Plexiglas chamber ($26\times26\times18$ cm) with a metal rod floor delivering a footshock (San Diego Instruments, San Diego, CA). The conditioned auditory stimulus was provided by a white noise generator (PLMR24, Pyle Audio Inc). A Dell Optiplex computer connected to the shock generator delivered the unconditioned foot shock stimulus (0.50-mA AC current). The novel context chamber used for scoring the cued fear conditioning consisted of a white plastic triangular shaped chamber ($36\times36\times51$ cm) with 26 cm high walls and a solid floor. The chamber was placed on the floor of a test room that differed from the training test room. A novel odor (1:10 diluted McCormick vanilla extract) was spread with a cotton-tipped applicator on one wall of the triangle prior to the start of each test session. Freezing was tracked by a digital video camera interfaced to a PC installed with ANYmaze. Mice were brought individually to the testing room, placed into the conditioning chamber, and presented with 3 pairings of auditory white noise (US) and foot shock (CS). The CS-US pairings were comprised of 30 s of white noise, a 2.5-s trace interval, and a 1-s footshock. Timing of the auditory cue presentation and foot shock delivery were coordinated through San Diego Instruments software. Freezing was scored during the initial 2 min period prior to the CS-US pairings and during the final 2 min. Twenty-four hours after training, mice were brought individually to the original test room and returned to the training chamber (same context), with the test room environment identical to the training day, for the contextual test. Mice were placed in the chamber and allowed to explore for 5 min in the absence of the auditory cue and foot shock. Freezing behavior was scored over the 5 min test period. Forty-eight hours post-training, mice were brought to a different test room and placed in the triangular chamber (novel context) for auditory cue testing. The session consisted of a 3 min exploration period (pre-cue period) followed by 30 s of exploration with the identical 80 dB white noise (cue period), then a 4 min period with no sound cue (post-cue period). *Rotarod.* The rotarod test of motor coordination and motor learning was performed 3 trials a day for two consecutive days by placing each mouse on a rotating drum (Accuscan, Columbus, OH) that accelerated from 4 to 40 rpm over a 5-min period. The latency to fall from the drum was the measure of motor coordination. Improvement across trials was the measure of motor learning. *Open field exploration.* Exploratory locomotor activity was assayed in an automated open field arena (Accuscan, Columbus, OH). Open field chambers consisted of clear Plexiglas sides and floor approximately $40\times40\times30.5$ cm. Mice were placed in the center of the open field and allowed to explore the chamber for 15 min. Horizontal activity, total distance, vertical activity, and center time were automatically collected using Anymaze software. *Moriss water maze.* Spatial learning and memory were assessed in the Morris water maze using

established procedures and equipment. The training sequence was a) acquisition of hidden platform, b) probe trial. The apparatus was a circular pool (120 cm diameter) filled 45 cm deep with tap water rendered opaque with the addition of non-toxic (Crayola) white paint. Trials were scored with ANYmaze. Training consisted of 4 trials per session per day. The mouse was placed into the pool facing the pool edge in a new quadrant for each trial. The hidden platform remained in the same quadrant for all trials across all sessions of acquisition. Training and trials lasted 60 s. During the training, if the mouse did not locate the platform within 60 s, it was guided to the platform by the experimenter. Subjects were left on the platform for 15 s before being placed under a warming light for the 30–45 s intertrial intervals. Hidden platform training continued until the control group met the criteria of 15 s or less latency to find the hidden platform.

Mice were tested on a 60 s probe trial 24 h after completing hidden platform testing on the day criteria was met. Parameters recorded during training were latency to reach the platform, total distance traveled, swim speed and thigmotaxis. Probe trial selective quadrant search was assessed by time and distance spent in each quadrant and the number of crossings over the trained quadrant platform location compared to the analogous locations in the non-trained quadrants.

2.3. Morphological study

The Ad-GFP-IL-6 and Ad-GFP mice, 12 weeks of age, were anesthetized and perfusion-fixed with 4% fresh paraformaldehyde and cryoprotected with 30% sucrose. 40 μm parasagittal cryostat sections were blocked with 3% goat serum/0.3% Triton X-100 in PBS and incubated with anti-Synaptophysin polyclonal antibody (1:200, Cell Signaling Technology), anti-VGLUT1 monoclonal antibody (1:500, Millipore), and anti-VGAT polyclonal antibody (1:500, Millipore) overnight at 4 °C, followed by incubation with Alexa Fluor 555 anti-mouse and anti-rabbit IgG (1:1000, Invitrogen) for 1.5 h at room temperature. Sections were transferred onto SuperFrost slides and mounted under glass coverslips with ProLong Gold antifade reagent (Invitrogen). Sections of hippocampus and somatosensory cortex were imaged with Nikon eclipse 90i confocal laser scanning microscope. For quantitative analysis, the CA1 and CA3 subfields of the hippocampus, and somatosensory cortex were imaged. Images were acquired in the linear range with constant settings and analyzed with ImageJ and normalized with data from Ad-GFP mice to determine synaptic density and size, respectively. All analyses were performed blind to the treatment of the animals. Immunoreactive puncta were defined as discrete regions along the dendrite with fluorescence intensity twice the background. Negative controls, in which the primary antibodies were omitted and treated only with the secondary antibodies, were run for each condition to exclude false positive secondary antibody binding.

2.4. DiI labeling of dendrites

DiI labeling was employed to outline the shape of dendritic spines, modified from the literatures [31,32]. The mice, 16 weeks of age, were transcardially perfused with 0.1 M PBS and followed by 1.5% paraformaldehyde in 0.1 M PBS for 30 min. Brains were removed and post-fixed in the same fixative for 1 h, and then were coronally sectioned

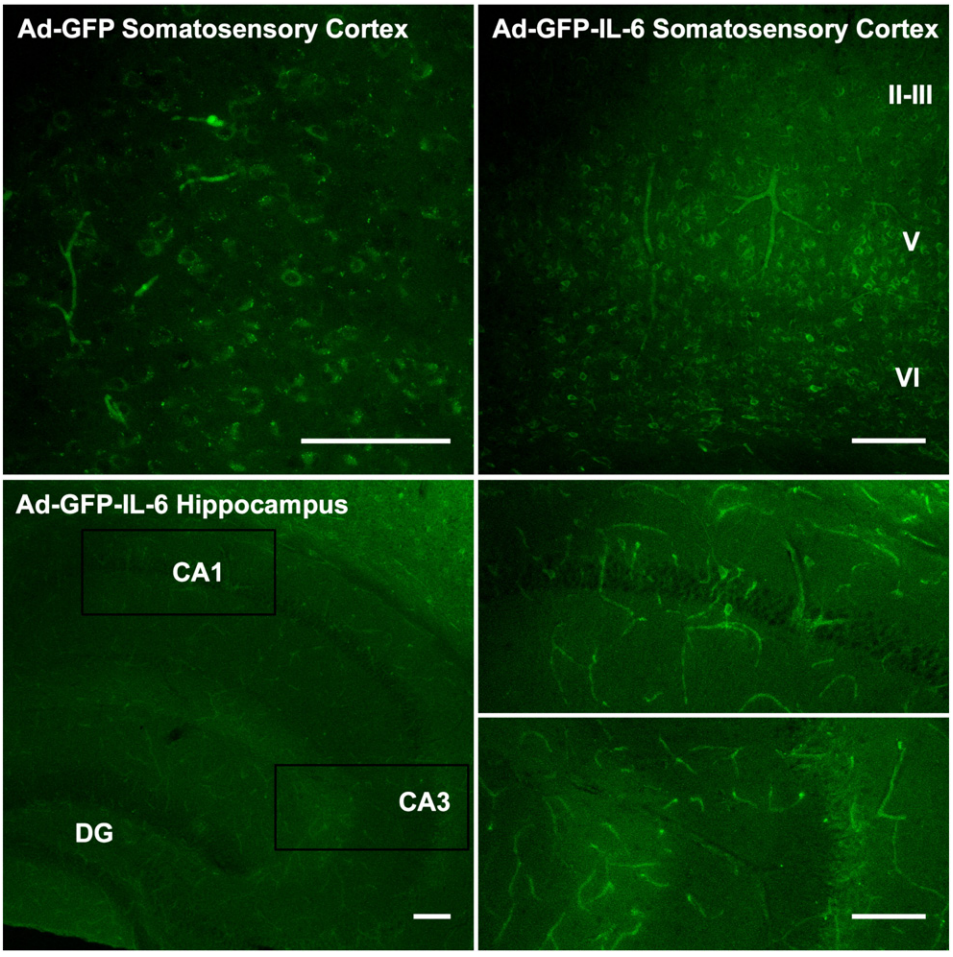

Fig. 1. Intracranial expression of GFP-IL-6 using adenovirus transduction in the brain. C57BL/6J pups (P0.5) were injected intracerebroventricularly with Ad-GFP or Ad-GFP-IL-6. The intracranial expression of GFP-IL-6 was examined at 12 weeks post injection. The expression was seen in the neuronal cell layers of hippocampal CA1 to CA3 region and somatosensory cortex. The right figures were the magnified areas from the boxes of the left figures. Scale bar, 100 μm.

(200 μm thick) using a vibratome at room temperature. Slices were incubated with Vybrant-DiI cell-labeling solution (1: 150, V22885, Invitrogen) for 36 h at 4 °C to allow DiI crystals to diffuse fully along the neuronal membranes. The slices were bathed in the PBS for 48 h to allow more time for diffusion. The slices were mounted on glass slides with ProLong Gold antifade reagent (Invitrogen). All images were taken within 7 days after coverslipping using Nikon eclipse 90i confocal laser scanning microscope.

Spine quantification and measurements were done as described previously [33,34]. Spines were counted by scrolling through the Z-stack and marking each spine. Spine density was computed as number of spines per dendrite length in 10 microns. Spine length was measured from shaft to tip using a bent-line tool on maximum intensity projections of the Z-stacks. To obtain spine area, image regions including head and neck, but not dendritic shaft, were measured and counted as the number of non-zero pixels and multiplied by the calibration factor. Spines with a minimum head diameter of 0.35 μm and minimum head vs neck ratio of 1.1 were classified as mushroom spines [35]. The spines were counted in 5–6 neurons/mouse and 3 mice/group. For each neuron, 3–5 dendrites were analyzed and the values were averaged within each individual neuron.

2.5. Hippocampal slice electrophysiology

The electrophysiology was done as described previously [36]. Animals, ~16 weeks of age, were anesthetized with CO_2 and decapitated. The brain was rapidly removed and immersed in ice-cold sucrose-based artificial CSF (sucrose-ACSF) (in mM: 126 sucrose, 5.0 KCl, 2.0 $CaCl_2$, 2.0 $MgSO_4$, 1.25 NaH_2PO_4, 26 $NaHCO_3$, and 10 D-glucose, pH 7.4). Slices containing both the hippocampus and adjacent entorhinal cortex (300 μm) were cut in the horizontal plane using a vibratome (*Leica*) and transferred to a nylon net in a recording chamber (Fine Science Tools, Foster City, CA) in which they were maintained at ~31 °C, oxygenated (5% CO_2, 95% O_2), and immersed in sucrose-ACSF, except for the upper surface. After 30 min, sucrose-ACSF was replaced by ACSF containing NaCl substituted equimolar for sucrose (saline-ACSF), and recordings began 30 min later. The recording chamber was continually perfused with saline-ACSF at a rate of ~1 ml/min, regulated by a peristaltic pump (Gilson, Middleton, WI). Recording electrodes made of borosilicate glass (0.75 mm inner diameter, 1.0 mm outer diameter; World Precision Instruments, Sarasota, FL) were pulled horizontally (Sutter Instruments, Novato, CA) and filled with saline-ACSF for extracellular recordings (10–15 MΩ resistance).

Monopolar stimulating electrodes were made from Teflon-coated wire (75 μm diameter, including Teflon; A-M Systems, Carlsborg, WA), and stimuli were triggered digitally (100 μA, 10–200 μs; STG1002 Stimulus generator, Multichannel systems) at low frequencies (<0.05 Hz). For Schaffer collateral activation of CA1 pyramidal cells, the stimulating electrode was placed at the tip of the Schaffer collateral bundle, on the border of CA2, ~150 μm from the pyramidal cell layer, and the recording site was CA1. The site ultimately used was the one in which the maximal response was elicited of all of those tested. Electrophysiological data were collected using an amplifier (HEKA Electronics, Lambrecht/Pfalz, Germany) and stored using IGOR Pro 6.2 software (WaveMetrics, Lake Oswego, OR).

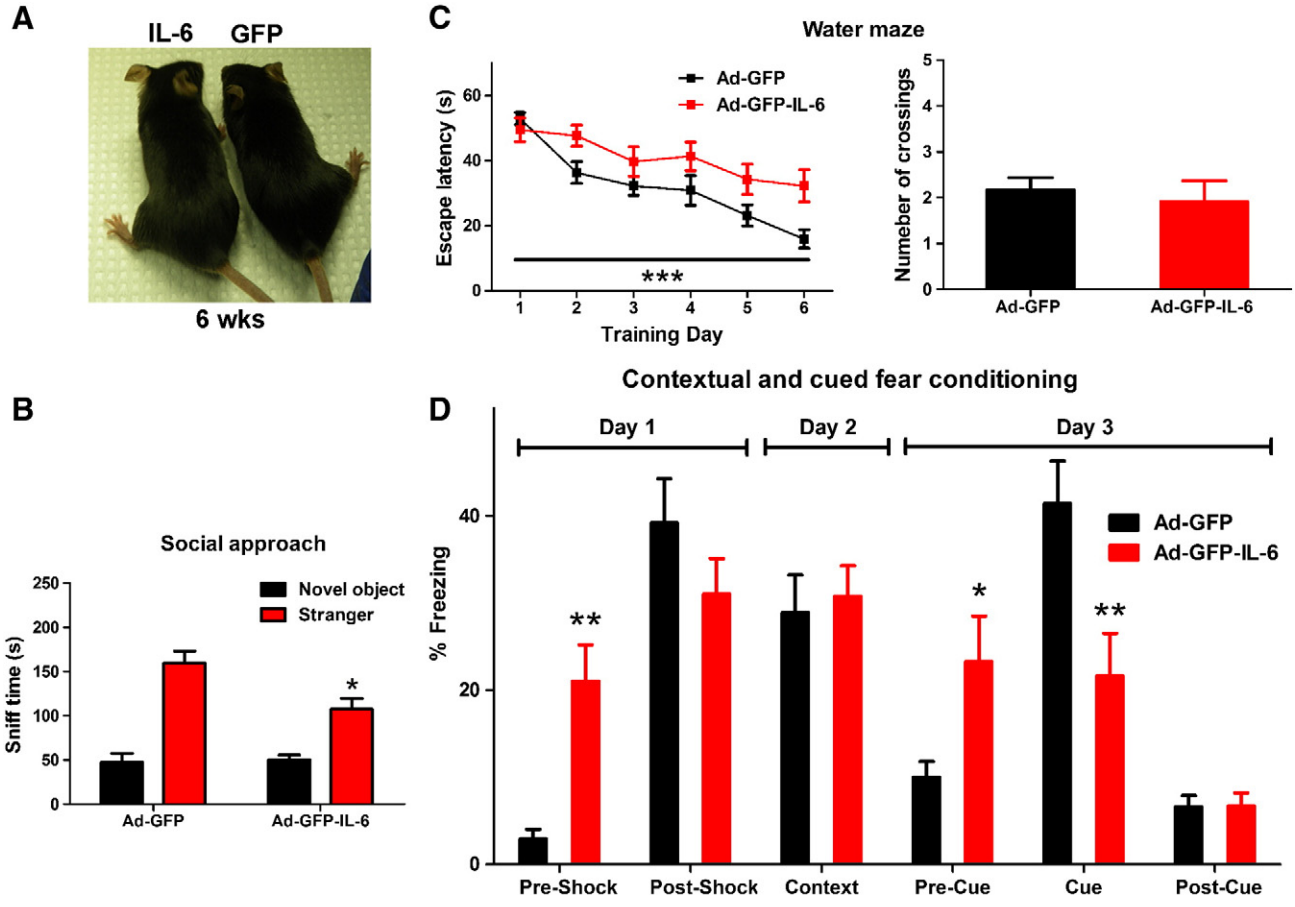

Fig. 2. Ad-GFP-IL-6 mice show decreased social interaction and impaired cognition capacity. (A) Ad-GFP-IL-6 mice had similar size with control mice at 6 wks. (B) Ad-GFP-IL-6 mice spent less time interacting with an stranger mouse than compared to controls at the age of 18 wks, n = 9. (C) Ad-GFP-IL-6 mice did not show improvement for latency to reach the hidden platform and showed a similar crossings over the target platform location during the probe test, n = 12. (D) Contextual and cued fear conditioning. Ad-GFP-IL-6 mice froze more before training but not following training. Ad-GFP-IL-6 mice and Ad-GFP mice did not differ in freezing to the identical context on Day 2. Ad-GFP-IL-6 mice demonstrated more freezing to the novel context (pre-cue) but significantly less freezing than Ad-GFP mice to the auditory cue (cue) on Day 3, n = 12. Values are mean ± SEM. *P<0.05, **P<0.01 and ***P<0.001.

The extracellularly recorded EPSP [field EPSP (fEPSP)] amplitude was measured as the voltage difference between the prestimulus potential and the peak of the fEPSP. To assess paired-pulse inhibition or paired-pulse facilitation, paired half-maximal stimuli were delivered to the Schaffer collateral pathway with a range of interstimulus intervals. Intervals of 10 and 20 ms were chosen to assess paired-pulse inhibition, whereas intervals of 40, 80 and 120 ms were chosen to assess paired-pulse facilitation, based on empirical determination that these intervals provided strong paired-pulse inhibition and robust facilitation, respectively. The paired-pulse ratio was defined as (amplitude evoked by the second stimulus)/(amplitude evoked by the first stimulus). All data acquisition and analysis was carried out blinded to treatments. Recordings were obtained from one mouse per day.

2.6. Statistics

All data were analyzed using commercially available statistical software packages (StatView 5.0 and GraphPad Prism 5). General health and neurological screening was analyzed using unpaired *t*-test (two-tailed). Elevated plus maze, social approach, fear conditioning, accelerating rotarod, open field test and Morris water maze were analyzed using two-way ANOVA with repeated measures with Bonferroni's post hoc comparison. The immunohistochemistry findings were analyzed with the unpaired *t* test (two-tailed). Spine density, spine length, spine area and ratio of mushroom spine were analyzed with unpaired *t*-test (two-tailed). The Kolmogorov–Smirnov test was used to compare the patterns of cumulative frequency. The paired pulse ratio data was analyzed by two-way ANOVA with repeated measures with Bonferroni's post hoc analysis. All data are shown as mean ± SEM. For all findings, the statistically significant *P* values are shown as $^{*}P<0.05$, $^{**}P<0.01$, and $^{***}P<0.001$.

3. Results

3.1. Generation and characterization of Ad-GFP-IL-6 mice

Injection of an adenovirus-gene construct into the cerebral ventricles of the mouse has been reported to result in widespread transduction and life-long expression of the packaged gene [37,38]. To develop a mouse model with stable over-expression of IL-6 in the brain, adenovirus encoding green fluorescent protein (GFP) IL-6 fusion protein (Ad-GFP-IL-6) and adenovirus encoding GFP (Ad-GFP) as control were bilaterally injected into the cerebral lateral ventricles of P0.5 C57BL/6J mice [39,40], GFP expression was detected as green fluorescence in brain slices 12 weeks after injection. The fluorescence was seen in the neuronal cell layers of hippocampal CA1 to CA3 region, somatosensory cortex (Fig. 1) and cerebellum (Supplementary Fig. 1) and even other cell types. The IL-6 gene was successfully delivered into the brain.

3.2. Ad-GFP-IL-6 mice with IL-6 overexpression in the brain show the autism-like features

3.2.1. Similar general health

Ad-GFP-IL-6 mice and control Ad-GFP mice were similar on most measures of general health, reflexes, and sensory function. The Ad-GFP-IL-6 mice showed the similar size and weight with control mice (Fig. 2A and Supplementary Table 1). General reactivity was assessed with petting escape, struggling and/or vocalizations, and dowel biting. There were no significant differences between two groups. Observations of home cage behaviors indicated that Ad-GFP-IL-6 mice were normal on home cage activity, nest building, huddling, and repetitive self-grooming. All reflexes were present in both groups. A group difference was detected in the wire hang test, in which the Ad-GFP mice hung on longer than did the Ad-GFP-IL-6 mice (Supplementary Table 1).

3.2.2. Impaired social approach behavior

The three-chambered sociability test showed that Ad-GFP-IL-6 mice showed significantly impaired social approach behavior as compared with the controls. Paired comparisons revealed that mice in both groups spent more time in the chamber of the stranger mouse (Supplementary Fig. 2), but the Ad-GFP-IL-6 mice spent significant less time sniffing the stranger mouse compared to the Ad-GFP group at 18-weeks ($P<0.05$; Fig. 2B).

3.2.3. Impaired cognitive ability

The Morris water maze (MWM) was used to investigate spatial learning and memory. MWM learning is thought to rely extensively on the hippocampus. Fig. 2C illustrates the performance of the two groups of mice in the MWM spatial learning and memory task. During acquisition, there was a significant main effect of IL-6 treatment ($P<0.001$), in which the Ad-GFP-IL-6 mice did not show improvement during six days of training for latency to reach the hidden platform. The Ad-GFP-IL-6 mice also swam a greater total distance compared to the Ad-GFP mice across the days of training ($P<0.05$; Supplementary Fig. 3A). The swimming speed did not differ between the two groups on any day of training (Supplementary Fig. 3B). During the probe trial, we did not find significant differences between the

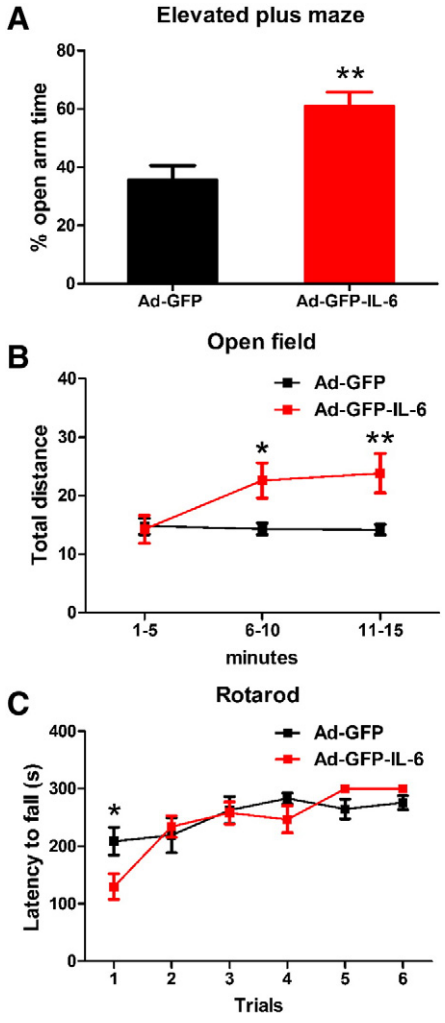

Fig. 3. Ad-GFP-IL-6 mice shown abnormal anxiety-like trait and habituation.(A) Ad-GFP-IL-6 mice spent more time on the open arms, n = 12. (B) Ad-GFP-IL-6 mice traveled longer distances during the open field test, n = 12. (C) Ad-GFP-IL-6 mice did not differ in latency to fall from the accelerating rotarod test, n = 12. Values are mean ± SEM. $^{*}P<0.05$, $^{**}P<0.01$.

two groups on platform crossings or time spent in the training quadrant (Fig. 2C and Supplementary Fig. 3C). We conclude that IL-6 affected acquisition of the task, but not performance during probe trials.

The mice were also assessed for learning and memory in a trace contextual and cued fear learning paradigm. As shown in Fig. 2D, in the training phase, there was no significant effect of treatment on freezing behavior following the tone-cue pairings, though the Ad-GFP-IL-6 mice froze more prior to training. Both groups showed significantly more freezing following training than in the initial 2 min before the tone-cue pairings. Treatment did not affect the time spent freezing during the context test on Day 2. On Day 3, the mice were placed in a novel environmental context and given the auditory tone that had been paired with footshock during training. The Ad-GFP-IL-6 mice demonstrated more freezing to the novel context but significantly less freezing than Ad-GFP mice to the auditory cue ($P<0.01$). Notably, the Ad-GFP-IL-6 mice froze significantly more pre-training on the first day and pre-cue in the novel context than Ad-GFP mice (Fig. 2D). During the first 2–3 minutes in a new

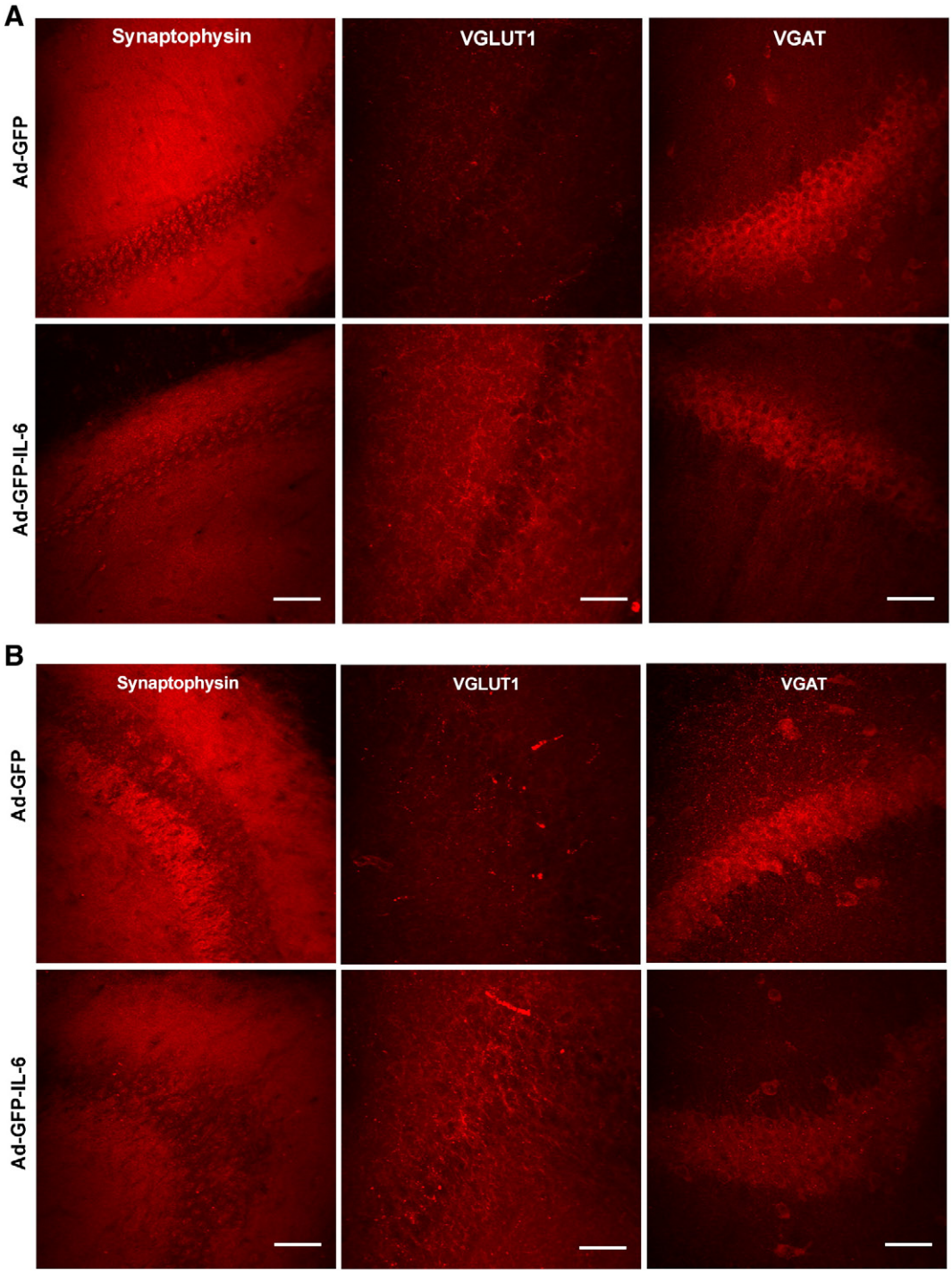

Fig. 4. Ad-GFP-IL-6 mice exhibit an increased excitatory synapse formation and a reduced inhibitory synapse formation. Representative confocal immunofluorescence images of sections of the CA1 region (A) and CA3 region (B) in the hippocampus and somatosensory cortex (C) from 3 Ad-GFP-IL-6 mice and 3 Ad-GFP mice after being labeled with antibodies to Synaptophysin (labels all synapses), VGLUT1 (labels excitatory synapses) and VGAT (labels inhibitory synapses). For each animal, at least three nonconsecutive sections were analyzed. Scale bar, 50 μm. The legend in one of the panels applies to all panels. D, Quantitation of the density of synaptic puncta that are above threshold by image analysis of confocal immunofluorescence sections. Values are mean ± SEM. $^{*}P<0.05$, $^{**}P<0.01$ and $^{***}P<0.001$.

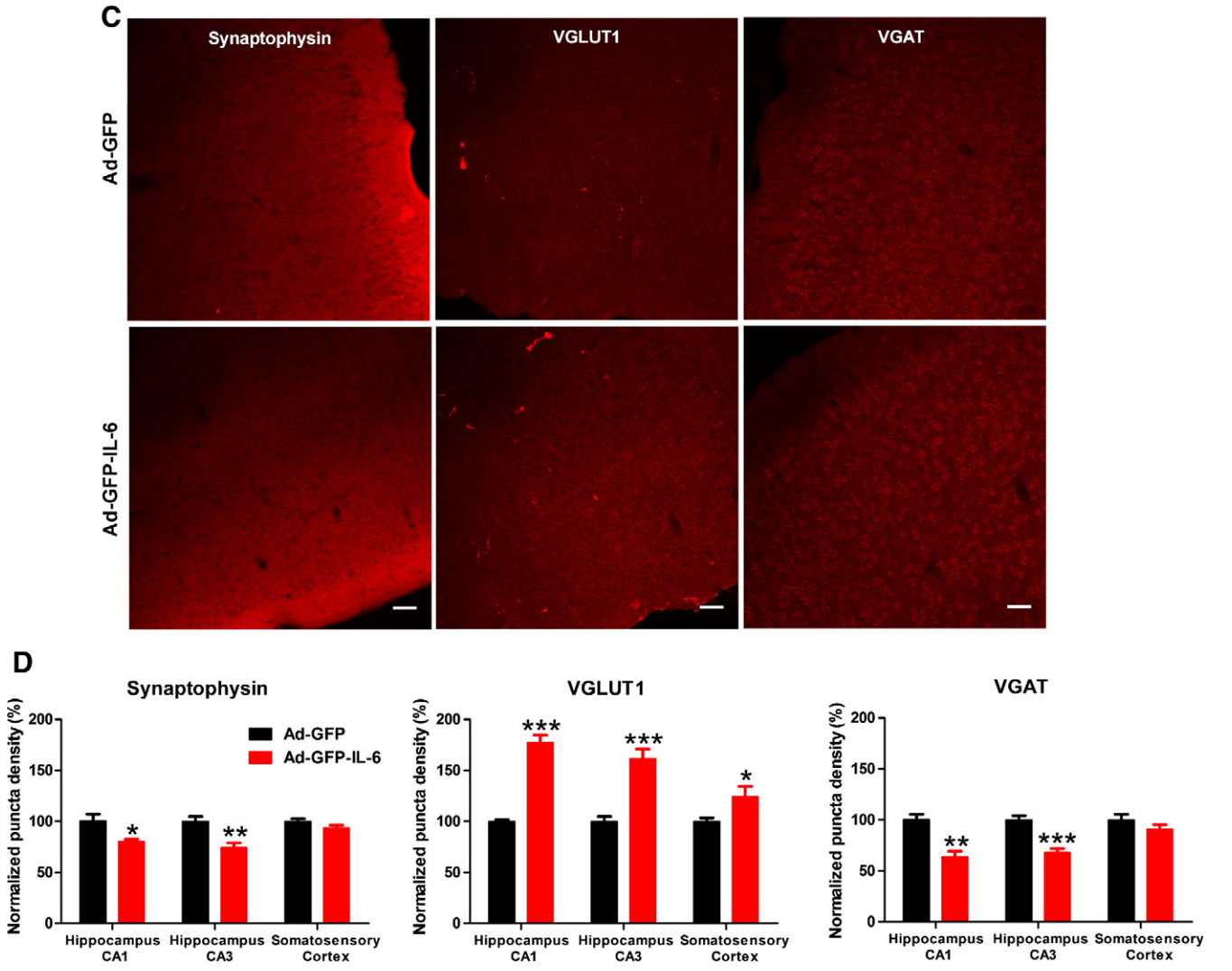

Fig. 4 (*continued*).

environment, the Ad-GFP-IL-6 mice spent less time exploring than the control mice indicating possible deficits in habituating to a novel environment. The data from the open field test in which the Ad-GFP-IL-6 mice increased their total distance traveled in the second and third 5 min intervals as compared with the controls (see below) seem to support this. Our results revealed that the elevated IL-6 in brain disrupted cued fear memory but did not affect contextual fear memory.

3.2.4. Abnormal anxiety-like trait and habituation

As shown in Fig. 3A, in the elevated plus maze test, Ad-GFP-IL-6 mice spent more time on the open arms ($P<0.01$), indicating that Ad-GFP-IL-6 mice exhibited less anxiety-like behavior. Next, we employed the open field test to examine whether Ad-GFP-IL-6 mice exhibit abnormal habituation. Habituation to an open field is measured as a change in exploratory activity over time [41]. During the open field test, Ad-GFP-IL-6 mice traveled longer distances during the second and third 5-min intervals, indicating that Ad-GFP-IL-6 mice have a defect in habituating to a novel environment (Fig. 3B). The increased traveling distance is not related to locomotor ability because the Ad-GFP-IL-6 mice did not have a difference in latency to fall from the accelerating rotarod test (Fig. 3C) as compared to Ad-GFP mice.

3.3. Ad-GFP-IL-6 mice exhibit an increase in excitatory synapse formation and a reduction in inhibitory synapse formation

A growing number of studies suggest that autism is likely to arise from functional changes in neural circuitry and to be associated with an imbalance between excitatory and inhibitory synaptic transmission, although the mechanisms involved are unclear [42-44]. To investigate whether IL-6 could mediate autism-like behaviors through its effects on neural circuitry, we examined the development of synapses in Ad-GFP-IL-6 and Ad-GFP mice by using antibodies to synaptic vesicle proteins. An antibody to synaptophysin, a general marker of all synapses, as well as antibodies to VGLUT1 (vesicular glutamate transporter), a marker of excitatory synapses, and VGAT (the vesicular GABA transporter), a marker of inhibitory synapses, were used in this study (Fig. 4A–C). By image analysis, we observed a dramatic increase in the intensity of VGLUT1 in Ad-GFP-IL-6 mice as compared with Ad-GFP mice in the hippocampus ($P<0.001$) and somatosensory cortex ($P<0.05$) (Fig. 4D). In contrast, the intensity of Synaptophysin and VGAT was decreased in the hippocampus but not in the somatosensory cortex. These data suggest that IL-6 over-expression may impair the balance of neural circuitry by stimulating the formation of excitatory synapses and reducing the formation of inhibitory synapses.

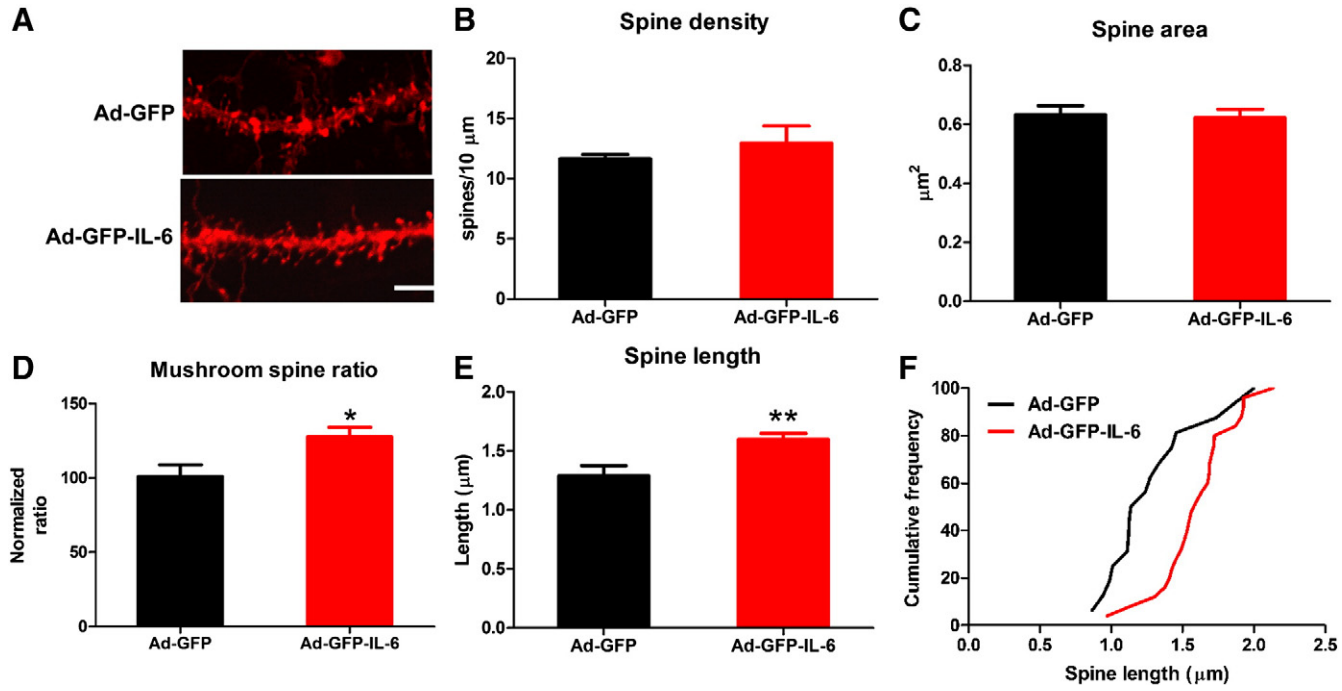

Fig. 5. Ad-GFP-IL-6 mice have larger numbers of mushroom-shaped dendritic spines and the length of spines are increased(A) Confocal micrographs of DiI labeled dendrites in cortex somatosensory layer from 3 Ad-GFP-IL-6 mice and 3 Ad-GFP mice. Scale bar, 5 μm. The legend applies to both panels. No significant differences were observed for spine density (B) and spine area (C) between the two groups. (D) Neurons in Ad-GFP-IL-6 mice had an abnormally high fraction of mushroom spines. (E) Spine length is increased in Ad-GFP-IL-6 mice. (F) Cumulative frequency distribution of spine lengths, corresponding to the dataset in (E). Values are mean ± SEM. $^{*}P<0.05$, $^{**}P<0.01$.

3.4. Ad-GFP-IL-6 mice have larger numbers of mushroom-shaped dendritic spines and the length of spines are increased

Dendritic spine dynamics plays an important role in mediating learning and memory, and is of essential importance to synaptic function [45-48]. Studies suggest that excitatory synapses mainly connect to mushroom-shaped dendritic spines [49]. It has also been shown that the size and length of dendritic spines are closely related to their functions. To further investigate whether IL-6 overexpression affected the development of dendritic spines, we employed DiI labeling to outline dendritic spines in pyramidal neurons of the somatosensory cortex (Fig. 5A). Our results showed that both the density and the size of dendritic spines were not altered in Ad-GFP-IL-6 mice as compared with the controls (Fig. 5, B and C). However, we found the Ad-GFP-IL-6 mice had significantly larger numbers of mushroom-shaped dendritic spines, while the total spine numbers remained unchanged. Fig. 5D shows that neurons in Ad-GFP-IL-6 mice had an abnormally high fraction of mushroom spines, identified by their head vs neck width ratios [35]. The spines with the mushroom morphology were increased by ~27% ($P<0.05$). Next we examined the effects of IL-6 on spine length and detected that the dendritic spines on average were 23% longer in Ad-GFP-IL-6 mice than in Ad-GFP mice ($P<0.01$; Fig. 5E). In addition, the distribution of different length of spines was altered ($P<0.01$; Fig. 5F). Ad-GFP-IL-6 mice have fewer short spines and more medium to long spines. Taken together, these data indicate that over-expression of IL-6 in mice brain can strongly affect the morphology of dendritic spines and impair the normal pattern of spine shape.

3.5. Reduced postexcitatory inhibition in Ad-GFP-IL-6 mice

A paired-pulse paradigm is commonly used to study postexcitatory inhibition effects related to synaptic processes and neurotransmitters release [50]. To further investigate whether the effect of IL-6 on synaptic proteins and drendrtic spines may lead to an alteration of synaptic transmission, we measured synaptic function in the Ad-GFP-IL-6 mice by recording extracellular field excitatory post-synaptic potentials (fEPSPs) in the CA1 area of the hippocampus in acute slices. Intervals of 10 and 20 ms were chosen to assess paired-pulse inhibition, whereas intervals of 40 and 80 ms were chosen to assess paired-pulse facilitation, based on empirical determinations that these intervals provide strong paired-pulse inhibition and robust facilitation, respectively [36]. Fig. 6A shows typical examples of paired-pulse responses recorded from Ad-GFP-IL-6 mice and Ad-GFP mice at different interstimulus intervals (ISI). Ad-GFP-IL-6 mice exhibited an increase in the paired-pulse ratio at the shorter ISIs of 10 and 20 ms, indicating a decrease in inhibition ($P<0.001$; Fig. 6B). The two groups showed no significant difference of paired-pulse ratios at the longer ISIs of 40, 80 and 120 ms, indicating that they have similar paired-pulse facilitation (Fig. 6B). Paired-pulse facilitation and paired-pulse inhibition have been considered to be forms of short-term synaptic plasticity [50]. We also tested the long-term potentiation (LTP) of fEPSPs, a form of long-term plasticity, which was induced after a 30 min period of stable baseline responses by applying a theta-burst stimulation (TBS) train. No significant difference was detected between the two groups (data not shown).

4. Discussion

A growing number of studies suggest that dysregulated immune responses may be involved in autism. Various hypotheses have attempted to link dysfunctional immune activity and autism, such as maternal immune abnormalities during early pregnancy, increased incidence of familial autoimmunity, and childhood vaccinations [7]. Recently several lines of research have shown increased expression of inflammatory cytokines in the peripheral blood, brain and cerebrospinal fluid of autistic subjects [7,10,12,13]. In particular, IL-6 elevation in the autistic brain has been a repeated finding [14,15,51]. IL-6

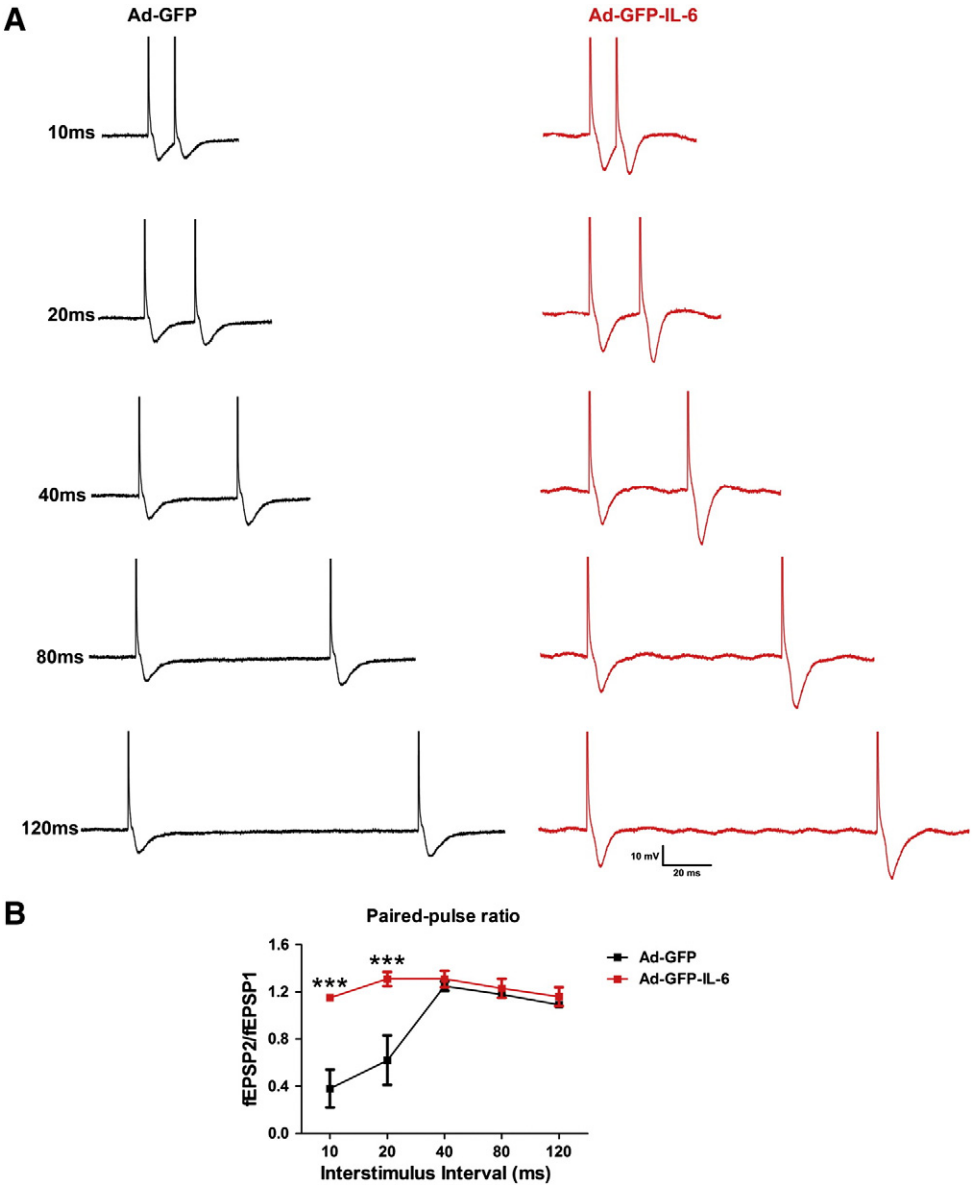

Fig. 6. Reduced postexcitatory inhibition in Ad-GFP-IL-6 mice. Paired-pulse ratio of fEPSP was measured in CA1 area of the hippocampus in response to the indicated inter-stimulus intervals. (A) Representative traces for multiple inter-stimulus intervals. (B) Summary graph of paired pulse ratio in 3 Ad-GFP-IL-6 mice and 3 Ad-GFP mice. Paired-pulse response is represented as the ratio of the second to first fEPSP amplitude. Data shown in summary graphs are mean ± SEM. ***$P<0.001$.

signaling has also been suggested as a key mechanistic pathway in maternal immune activation that may be associated with autism [52]. In the CNS, the cellular sources of IL-6 include astrocytes, microglia and neurons [22,53]. IL-6 is normally expressed at relatively low levels and increases under pathological condition [53,54]. However whether the increased IL-6 expression found in the autistic brain has specific behavioral consequences remains unknown. In this study, we developed a mouse model for over-expressing IL-6 in the brain with an adenoviral gene delivery approach. We demonstrated that IL-6 is an important mediator of autism-like behaviors. Mice with an elevated IL-6 in brain developed autism-like behaviors, including impaired cognition ability, deficits in learning, abnormal anxiety-like trait and habituation, as well as a decreased social interaction initiated at later stages. These findings suggest that an IL-6 elevation in the brain could modulate certain pathological alterations and contribute to the development of autism.

Inhibitory and excitatory synapses play fundamental roles in information processing in the brain. Inappropriate loss of synaptic stability could lead to the disruption of neuronal circuits and to brain dysfunction. The possibility that alteration of synaptic functions could lead to autism was noted by the phenotypic overlap between autism, fragile X syndrome, and Rett syndrome [55,56]. A key role for excitatory/inhibitory alterations in autism is supported by the observation that 10–30% of autistic individuals have epilepsy [57]. The synaptic abnormality hypothesis is further supported by the identification of mutations affecting synaptic cell adhesion molecules, including NRXN1, NLGN3/4, SHANK3, as well as mutations in synaptic proteins, including CNTNAP2, CACNA1C, CNTN3/4 and PCDH9/10, in autistic subjects [1,58-65]. To further investigate the possible mechanisms through which IL-6 elevation may mediate autistic phenotypes, we examined whether IL-6 over-expression affected synaptic protein development and neural circuit balances. We detected that an IL-6 elevation stimulated excitatory synapse formation, but impaired the development of inhibitory synapses. The complexity and specificity of synaptogenesis relies upon modulation of cell adhesion molecules (CAMs), which regulate contact initiation, synapse formation,

maturation, and functional plasticity. Disruption of adhesion may result in structural and functional imbalances at synapses. A recent study in our lab found that IL-6 overexpression in cultured mice cerebellar granule cells impaired cell adhesion and migration [51]. This finding may suggest that IL-6 could be involved in the regulation of CAMs. It will be of interest for future studies to determine whether the effect of IL-6 on synapse formation is through its possible modulation of CAMs.

Dendritic spines are small membranous protrusions that contain the postsynaptic machinery, including glutamate receptors, postsynaptic densities (PSD), the actin cytoskeleton, and a wide variety of membrane-bound organelles, such as smooth endoplasmic reticulum, mitochondria, and endosomes. Electron microscopic studies have identified several categories of spines based on their shape and size, including thin, stubby, cup, and mushroom shaped [66]. It is becoming evident that spine morphology is intimately linked to synapse function, which is the basis of learning and memory [67]. In this study, we found that IL-6 elevation in mouse brain resulted in a significant increase in the length of dendritic spines. In addition, IL-6 elevation stimulated the formation of mushroom-shaped dendritic spines, while the total numbers of spines remained unchanged. Increased spine length has been suggested to reflect a lag in the maturation of synaptic structures [68]. In addition, increased spine length has been reported in *Fmr1* knock-out mice, the animal model for the fragile X syndrome, and is also an animal model for autism, since about one third of patients with fragile X syndrome exhibit autism symptoms [68,69]. It is unknown whether abnormal development of dendritic spine is presented in autism. However our findings imply that an IL-6 elevation in the autistic brain could impair the maturation of dendritic spines.

Excitatory synapses are mainly situated on mushroom-shaped spines that have larger PSDs with a higher density of glutamate receptors [49,70,71]. The increased mushroom-shaped spines found in Ad-GFP-IL-6 mice thus further support the possibility that IL-6 elevation may stimulate the formation of excitatory synapses and result in enhanced excitatory synaptic transmission. It was reported that both the mRNA and protein levels of the AMPA glutamate receptor were significantly increased in the autistic brain [72]. We suggest that an IL-6 elevation may contribute to this alteration through its stimulating effect on the formation of mushroom-shaped spines that have a higher density of glutamate receptors. Taking together, our findings suggest that an IL-6 elevation could impair dendritic spine maturation/function and cause excitatory/inhibitory imbalances, which may be responsible for the learning and cognitive defects we observed in Ad-GFP-IL-6 mice.

To further investigate how IL-6 elevation affected the balance of excitatory and inhibitory processes, we recorded fEPSPs in the CA1 area of the hippocampus in acute slices. We detected a reduced postexcitatory inhibition in Ad-GFP-IL-6 mice. Postexcitatory inhibition analyzed by paired-pulse inhibition (PPI) has been suggested to be caused by a decrease in the release of excitatory neurotransmitters from terminals of afferent axons [73–75]. This effect is likely the result of an inhibition of calcium influx through presynaptic receptors which play a causal role in the release of glutamate from synaptic vesicles on afferent stimulation [50,76]. Thus, the reduced PPI in Ad-GFP-IL-6 mice indicates an increased release of excitatory neurotransmitters possibly stimulated by calcium influx. Orellana et al. [77] demonstrated that IL-6 treatment of rat hippocampal neurons increases the calcium influx via the NMDA-receptor and is mediated by the JAKs/STATs pathway. We suggest that IL-6 elevation in mouse brain could cause a reduced PPI through increasing calcium influx and stimulating the release of excitatory neurotanmitters. Decreased PPI has also been shown in some other neurological and psychiatric diseases including Huntington's disease, schizophrenia and in Down's syndrome [50]. Several lines of research have presented convincing data demonstrating an association between defects in inhibitory capacity and cognitive impairment [50,78].

In summary, our study supports a critical role of IL-6 elevation in modulating autism-like behaviors through impairments on synapse formation, dendritic spine development, as well as on neuronal circuit balance. These findings suggest that manipulation of IL-6 may be a promising avenue for therapeutic interventions.

Conflict of interest

The authors declare no conflict of interest.

Acknowledgements

This work was supported by the NYS Office for People with Developmental Disabilities, the Rural India Charitable Trust and Northfield Bank Foundation.

Appendix A. Supplementary data

Supplementary data to this article can be found online at doi:10.1016/j.bbadis.2012.01.011.

References

[1] B.S. Abrahams, D.H. Geschwind, Advances in autism genetics: on the threshold of a new neurobiology, Nat. Rev. Genet. 9 (2008) 341–355.
[2] J.D. Buxbaum, S. Baron-Cohen, B. Devlin, Genetics in psychiatry: common variant association studies, Mol. Autism 1 (2010) 6.
[3] B. Devlin, N. Melhem, K. Roeder, Do common variants play a role in risk for autism? Evidence and theoretical musings, Brain Res. 1380 (2011) 78–84.
[4] J. Hallmayer, S. Cleveland, A. Torres, J. Phillips, B. Cohen, T. Torigoe, J. Miller, A. Fedele, J. Collins, K. Smith, L. Lotspeich, L.A. Croen, S. Ozonoff, C. Lajonchere, J.K. Grether, N. Risch, Genetic heritability and shared environmental factors among twin pairs with autism, Arch. Gen. Psychiatry 68 (2011) 1095–1102.
[5] L.A. Weiss, Autism genetics: emerging data from genome-wide copy-number and single nucleotide polymorphism scans, Expert. Rev. Mol. Diagn. 9 (2009) 795–803.
[6] P. Ashwood, S. Wills, J. Van de Water, The immune response in autism: a new frontier for autism research, J. Leukoc. Biol. 80 (2006) 1–15.
[7] P. Ashwood, A.J. Wakefield, Immune activation of peripheral blood and mucosal CD3+ lymphocyte cytokine profiles in children with autism and gastrointestinal symptoms, J. Neuroimmunol. 173 (2006) 126–134.
[8] H. Jyonouchi, S. Sun, H. Le, Proinflammatory and regulatory cytokine production associated with innate and adaptive immune responses in children with autism spectrum disorders and developmental regression, J. Neuroimmunol. 120 (2001) 170–179.
[9] H. Jyonouchi, S. Sun, N. Itokazu, Innate immunity associated with inflammatory responses and cytokine production against common dietary proteins in patients with autism spectrum disorder, Neuropsychobiology 46 (2002) 76–84.
[10] V.K. Singh, Plasma increase of interleukin-12 and interferon-gamma. Pathological significance in autism, J. Neuroimmunol. 66 (1996) 143–145.
[11] J. Croonenberghs, E. Bosmans, D. Deboutte, G. Kenis, M. Maes, Activation of the inflammatory response system in autism, Neuropsychobiology 45 (2002) 1–6.
[12] C.A. Molloy, A.L. Morrow, J. Meinzen-Derr, K. Schleifer, K. Dienger, P. Manning-Courtney, M. Altaye, M. Wills-Karp, Elevated cytokine levels in children with autism spectrum disorder, J. Neuroimmunol. 172 (2006) 198–205.
[13] M.G. Chez, T. Dowling, P.B. Patel, P. Khanna, M. Kominsky, Elevation of tumor necrosis factor-alpha in cerebrospinal fluid of autistic children, Pediatr. Neurol. 36 (2007) 361–365.
[14] D.L. Vargas, C. Nascimbene, C. Krishnan, A.W. Zimmerman, C.A. Pardo, Neuroglial activation and neuroinflammation in the brain of patients with autism, Ann. Neurol. 57 (2005) 67–81.
[15] X. Li, A. Chauhan, A.M. Sheikh, S. Patil, V. Chauhan, X.M. Li, L. Ji, T. Brown, M. Malik, Elevated immune response in the brain of autistic patients, J. Neuroimmunol. 207 (2009) 111–116.
[16] I.L. Campbell, C.R. Abraham, E. Masliah, P. Kemper, J.D. Inglis, M.B. Oldstone, L. Mucke, Neurologic disease induced in transgenic mice by cerebral overexpression of interleukin 6, Proc. Natl. Acad. Sci. U. S. A. 90 (1993) 10061–10065.
[17] S.C. Steffensen, I.L. Campbell, S.J. Henriksen, Site-specific hippocampal pathophysiology due to cerebral overexpression of interleukin-6 in transgenic mice, Brain Res. 652 (1994) 149–153.
[18] M. Nakanishi, T. Niidome, S. Matsuda, A. Akaike, T. Kihara, H. Sugimoto, Microglia-derived interleukin-6 and leukaemia inhibitory factor promote astrocytic differentiation of neural stem/progenitor cells, Eur. J. Neurosci. 25 (2007) 649–658.
[19] J. Oh, M.A. McCloskey, C.C. Blong, L. Bendickson, M. Nilsen-Hamilton, D.S. Sakaguchi, Astrocyte-derived interleukin-6 promotes specific neuronal differentiation of neural progenitor cells from adult hippocampus, J. Neurosci. Res. 88 (2010) 2798–2809.
[20] P. Zhang, J. Chebath, P. Lonai, M. Revel, Enhancement of oligodendrocyte differentiation from murine embryonic stem cells by an activator of gp130 signaling, Stem Cells 22 (2004) 344–354.

[21] P.L. Zhang, A.M. Levy, L. Ben-Simchon, S. Haggiag, J. Chebath, M. Revel, Induction of neuronal and myelin-related gene expression by IL-6-receptor/IL-6: a study on embryonic dorsal root ganglia cells and isolated Schwann cells, Exp. Neurol. 208 (2007) 285–296.
[22] E.N. Benveniste, Cytokine actions in the central nervous system, Cytokine Growth Factor Rev. 9 (1998) 259–275.
[23] A.M. Samuelsson, E. Jennische, H.A. Hansson, A. Holmang, Prenatal exposure to interleukin-6 results in inflammatory neurodegeneration in hippocampus with NMDA/GABA(A) dysregulation and impaired spatial learning, Am. J. Physiol. Regul. Integr. Comp. Physiol. 290 (2006) R1345–R1356.
[24] S.M. Conroy, V. Nguyen, L.A. Quina, P. Blakely-Gonzales, C. Ur, J.G. Netzeband, A.L. Prieto, D.L. Gruol, Interleukin-6 produces neuronal loss in developing cerebellar granule neuron cultures, J. Neuroimmunol. 155 (2004) 43–54.
[25] Y.P. Peng, Y.H. Qiu, J.H. Lu, J.J. Wang, Interleukin-6 protects cultured cerebellar granule neurons against glutamate-induced neurotoxicity, Neurosci. Lett. 374 (2005) 192–196.
[26] X.C. Wang, Y.H. Qiu, Y.P. Peng, Interleukin-6 protects cerebellar granule neurons from NMDA-induced neurotoxicity, Sheng Li Xue Bao 59 (2007) 150–156.
[27] X.Q. Wang, Y.P. Peng, J.H. Lu, B.B. Cao, Y.H. Qiu, Neuroprotection of interleukin-6 against NMDA attack and its signal transduction by JAK and MAPK, Neurosci. Lett. 450 (2009) 122–126.
[28] S.E. Smith, J. Li, K. Garbett, K. Mirnics, P.H. Patterson, Maternal immune activation alters fetal brain development through interleukin-6, J. Neurosci. 27 (2007) 10695–10702.
[29] K.K. Chadman, Fluoxetine but not risperidone increases sociability in the BTBR mouse model of autism, Pharmacol. Biochem. Behav. 97 (2011) 586–594.
[30] K.K. Chadman, S. Gong, M.L. Scattoni, S.E. Boltuck, S.U. Gandhy, N. Heintz, J.N. Crawley, Minimal aberrant behavioral phenotypes of neuroligin-3 R451C knockin mice, Autism Res. 1 (2008) 147–158.
[31] H. Hering, C.C. Lin, M. Sheng, Lipid rafts in the maintenance of synapses, dendritic spines, and surface AMPA receptor stability, J. Neurosci. 23 (2003) 3262–3271.
[32] B.G. Kim, H.N. Dai, M. McAtee, S. Vicini, B.S. Bregman, Labeling of dendritic spines with the carbocyanine dye DiI for confocal microscopic imaging in lightly fixed cortical slices, J. Neurosci. Methods 162 (2007) 237–243.
[33] J. Jaworski, L.C. Kapitein, S.M. Gouveia, B.R. Dortland, P.S. Wulf, I. Grigoriev, P. Camera, S.A. Spangler, P. Di Stefano, J. Demmers, H. Krugers, P. Defilippi, A. Akhmanova, C.C. Hoogenraad, Dynamic microtubules regulate dendritic spine morphology and synaptic plasticity, Neuron 61 (2009) 85–100.
[34] H.W. Shen, S. Toda, K. Moussawi, A. Bouknight, D.S. Zahm, P.W. Kalivas, Altered dendritic spine plasticity in cocaine-withdrawn rats, J. Neurosci. 29 (2009) 2876–2884.
[35] A. Belly, G. Bodon, B. Blot, A. Bouron, R. Sadoul, Y. Goldberg, CHMP2B mutants linked to frontotemporal dementia impair maturation of dendritic spines, J. Cell Sci. 123 (2010) 2943–2954.
[36] D.P. McCloskey, S.D. Croll, H.E. Scharfman, Depression of synaptic transmission by vascular endothelial growth factor in adult rat hippocampus and evidence for increased efficacy after chronic seizures, J. Neurosci. 25 (2005) 8889–8897.
[37] S.O. Yoon, C. Lois, M. Alvirez, A. Alvarez-Buylla, E. Falck-Pedersen, M.V. Chao, Adenovirus-mediated gene delivery into neuronal precursors of the adult mouse brain, Proc. Natl. Acad. Sci. U. S. A. 93 (1996) 11974–11979.
[38] J.S. Shen, X.L. Meng, H. Maeda, T. Ohashi, Y. Eto, Widespread gene transduction to the central nervous system by adenovirus in utero: implication for prenatal gene therapy to brain involvement of lysosomal storage disease, J. Gene Med. 6 (2004) 1206–1215.
[39] Y. Levites, K. Jansen, L.A. Smithson, R. Dakin, V.M. Holloway, P. Das, T.E. Golde, Intracranial adeno-associated virus-mediated delivery of anti-pan amyloid beta, amyloid beta40, and amyloid beta42 single-chain variable fragments attenuates plaque pathology in amyloid precursor protein mice, J. Neurosci. 26 (2006) 11923–11928.
[40] M.A. Passini, J.H. Wolfe, Widespread gene delivery and structure-specific patterns of expression in the brain after intraventricular injections of neonatal mice with an adeno-associated virus vector, J. Virol. 75 (2001) 12382–12392.
[41] V.J. Bolivar, B.J. Caldarone, A.A. Reilly, L. Flaherty, Habituation of activity in an open field: A survey of inbred strains and F1 hybrids, Behav. Genet. 30 (2000) 285–293.
[42] J.L. Rubenstein, M.M. Merzenich, Model of autism: increased ratio of excitation/inhibition in key neural systems, Genes Brain Behav. 2 (2003) 255–267.
[43] K. Tabuchi, J. Blundell, M.R. Etherton, R.E. Hammer, X. Liu, C.M. Powell, T.C. Sudhof, A neuroligin-3 mutation implicated in autism increases inhibitory synaptic transmission in mice, Science 318 (2007) 71–76.
[44] T. Bourgeron, A synaptic trek to autism, Curr. Opin. Neurobiol. 19 (2009) 231–234.
[45] B. Calabrese, M.S. Wilson, S. Halpain, Development and regulation of dendritic spine synapses, Physiology (Bethesda) 21 (2006) 38–47.
[46] P. Hotulainen, C.C. Hoogenraad, Actin in dendritic spines: connecting dynamics to function, J. Cell Biol. 189 (2010) 619–629.
[47] H. Kasai, M. Fukuda, S. Watanabe, A. Hayashi-Takagi, J. Noguchi, Structural dynamics of dendritic spines in memory and cognition, Trends Neurosci. 33 (2010) 121–129.
[48] E.A. Nimchinsky, B.L. Sabatini, K. Svoboda, Structure and function of dendritic spines, Annu. Rev. Physiol. 64 (2002) 313–353.
[49] M. van Spronsen, C.C. Hoogenraad, Synapse pathology in psychiatric and neurologic disease, Curr. Neurol. Neurosci. Rep. 10 (2010) 207–214.
[50] E. Lukhanina, N. Berezetskaya, I. Karaban, Paired-pulse inhibition in the auditory cortex in Parkinson's disease and its dependence on clinical characteristics of the patients, Park. Dis. 2011 (2010) 342151.
[51] H. Wei, H. Zou, A. Sheikh, M. Malik, C. Dobkin, T. Brown, X. Li, IL-6 is increased in the cerebellum of the autistic brain and alters neural cell adhesion, migration and synapse formation, J. Neuroinflammation 8 (2011) 52.
[52] E.C. Parker-Athill, J. Tan, Maternal immune activation and autism spectrum disorder: interleukin-6 signaling as a key mechanistic pathway, Neurosignals 18 (2010) 113–128.
[53] E. Juttler, V. Tarabin, M. Schwaninger, Interleukin-6 (IL-6): a possible neuromodulator induced by neuronal activity, Neuroscientist 8 (2002) 268–275.
[54] R.A. Gadient, U.H. Otten, Interleukin-6 (IL-6)—a molecule with both beneficial and destructive potentials, Prog. Neurobiol. 52 (1997) 379–390.
[55] H.Y. Zoghbi, Postnatal neurodevelopmental disorders: meeting at the synapse? Science 302 (2003) 826–830.
[56] M.K. Belmonte, T. Bourgeron, Fragile X syndrome and autism at the intersection of genetic and neural networks, Nat. Neurosci. 9 (2006) 1221–1225.
[57] R. Canitano, Epilepsy in autism spectrum disorders, Eur. Child Adolesc. Psychiatry 16 (2007) 61–66.
[58] C.M. Durand, C. Betancur, T.M. Boeckers, J. Bockmann, P. Chaste, F. Fauchereau, G. Nygren, M. Rastam, I.C. Gillberg, H. Anckarsater, E. Sponheim, H. Goubran-Botros, R. Delorme, N. Chabane, M.C. Mouren-Simeoni, P. de Mas, E. Bieth, B. Roge, D. Heron, L. Burglen, C. Gillberg, M. Leboyer, T. Bourgeron, Mutations in the gene encoding the synaptic scaffolding protein SHANK3 are associated with autism spectrum disorders, Nat. Genet. 39 (2007) 25–27.
[59] P. Szatmari, A.D. Paterson, L. Zwaigenbaum, W. Roberts, J. Brian, X.Q. Liu, J.B. Vincent, J.L. Skaug, A.P. Thompson, L. Senman, L. Feuk, C. Qian, S.E. Bryson, M.B. Jones, C.R. Marshall, S.W. Scherer, V.J. Vieland, C. Bartlett, L.V. Mangin, R. Goedken, A. Segre, M.A. Pericak-Vance, M.L. Cuccaro, J.R. Gilbert, H.H. Wright, R.K. Abramson, C. Betancur, T. Bourgeron, C. Gillberg, M. Leboyer, J.D. Buxbaum, K.L. Davis, E. Hollander, J.M. Silverman, J. Hallmayer, L. Lotspeich, J.S. Sutcliffe, J.L. Haines, S.E. Folstein, J. Piven, T.H. Wassink, V. Sheffield, D.H. Geschwind, M. Bucan, W.T. Brown, R.M. Cantor, J.N. Constantino, T.C. Gilliam, M. Herbert, C. Lajonchere, D.H. Ledbetter, C. Lese-Martin, J. Miller, S. Nelson, C.A. Samango-Sprouse, S. Spence, M. State, R.E. Tanzi, H. Coon, G. Dawson, B. Devlin, A. Estes, P. Flodman, L. Klei, W.M. McMahon, N. Minshew, J. Munson, E. Korvatska, P.M. Rodier, G.D. Schellenberg, M. Smith, M.A. Spence, C. Stodgell, P.G. Tepper, E.M. Wijsman, C.E. Yu, B. Roge, C. Mantoulan, K. Wittemeyer, A. Poustka, B. Felder, S.M. Klauck, C. Schuster, F. Poustka, S. Bolte, S. Feineis-Matthews, E. Herbrecht, G. Schmotzer, J. Tsiantis, K. Papanikolaou, E. Maestrini, E. Bacchelli, F. Blasi, S. Carone, C. Toma, H. Van Engeland, M. de Jonge, C. Kemner, F. Koop, M. Langemeijer, C. Hijmans, W.G. Staal, G. Baird, P.F. Bolton, M.L. Rutter, E. Weisblatt, J. Green, C. Aldred, J.A. Wilkinson, A. Pickles, A. Le Couteur, T. Berney, H. McConachie, A.J. Bailey, K. Francis, G. Honeyman, A. Hutchinson, J.R. Parr, S. Wallace, A.P. Monaco, G. Barnby, K. Kobayashi, J.A. Lamb, I. Sousa, N. Sykes, E.H. Cook, S.J. Guter, B.L. Leventhal, J. Salt, C. Lord, C. Corsello, V. Hus, D.E. Weeks, F. Volkmar, M. Tauber, E. Fombonne, A. Shih, K.J. Meyer, Mapping autism risk loci using genetic linkage and chromosomal rearrangements, Nat. Genet. 39 (2007) 319–328.
[60] H.G. Kim, S. Kishikawa, A.W. Higgins, I.S. Seong, D.J. Donovan, Y. Shen, E. Lally, L.A. Weiss, J. Najm, K. Kutsche, M. Descartes, L. Holt, S. Braddock, R. Troxell, L. Kaplan, F. Volkmar, A. Klin, K. Tsatsanis, D.J. Harris, I. Noens, D.L. Pauls, M.J. Daly, M.E. MacDonald, C.C. Morton, B.J. Quade, J.F. Gusella, Disruption of neurexin 1 associated with autism spectrum disorder, Am. J. Hum. Genet. 82 (2008) 199–207.
[61] B. Bakkaloglu, B.J. O'Roak, A. Louvi, A.R. Gupta, J.F. Abelson, T.M. Morgan, K. Chawarska, A. Klin, A.G. Ercan-Sencicek, A.A. Stillman, G. Tanriover, B.S. Abrahams, J.A. Duvall, E.M. Robbins, D.H. Geschwind, T. Biederer, M. Gunel, R.P. Lifton, M.W. State, Molecular cytogenetic analysis and resequencing of contactin associated protein-like 2 in autism spectrum disorders, Am. J. Hum. Genet. 82 (2008) 165–173.
[62] M. Alarcon, B.S. Abrahams, J.L. Stone, J.A. Duvall, J.V. Perederiy, J.M. Bomar, J. Sebat, M. Wigler, C.L. Martin, D.H. Ledbetter, S.F. Nelson, R.M. Cantor, D.H. Geschwind, Linkage, association, and gene-expression analyses identify CNTNAP2 as an autism-susceptibility gene, Am. J. Hum. Genet. 82 (2008) 150–159.
[63] D.E. Arking, D.J. Cutler, C.W. Brune, T.M. Teslovich, K. West, M. Ikeda, A. Rea, M. Guy, S. Lin, E.H. Cook, A. Chakravarti, A common genetic variant in the neurexin superfamily member CNTNAP2 increases familial risk of autism, Am. J. Hum. Genet. 82 (2008) 160–164.
[64] C.R. Marshall, A. Noor, J.B. Vincent, A.C. Lionel, L. Feuk, J. Skaug, M. Shago, R. Moessner, D. Pinto, Y. Ren, B. Thiruvahindrapduram, A. Fiebig, S. Schreiber, J. Friedman, C.E. Ketelaars, Y.J. Vos, C. Ficicioglu, S. Kirkpatrick, R. Nicolson, L. Sloman, A. Summers, C.A. Gibbons, A. Teebi, D. Chitayat, R. Weksberg, A. Thompson, C. Vardy, V. Crosbie, S. Luscombe, R. Baatjes, L. Zwaigenbaum, W. Roberts, B. Fernandez, P. Szatmari, S.W. Scherer, Structural variation of chromosomes in autism spectrum disorder, Am. J. Hum. Genet. 82 (2008) 477–488.
[65] E.M. Morrow, S.Y. Yoo, S.W. Flavell, T.K. Kim, Y. Lin, R.S. Hill, N.M. Mukaddes, S. Balkhy, G. Gascon, A. Hashmi, S. Al-Saad, J. Ware, R.M. Joseph, R. Greenblatt, D. Gleason, J.A. Ertelt, K.A. Apse, A. Bodell, J.N. Partlow, B. Barry, H. Yao, K. Markianos, R.J. Ferland, M.E. Greenberg, C.A. Walsh, Identifying autism loci and genes by tracing recent shared ancestry, Science 321 (2008) 218–223.
[66] J.N. Bourne, K.M. Harris, Balancing structure and function at hippocampal dendritic spines, Annu. Rev. Neurosci. 31 (2008) 47–67.
[67] R. Yuste, T. Bonhoeffer, Morphological changes in dendritic spines associated with long-term synaptic plasticity, Annu. Rev. Neurosci. 24 (2001) 1071–1089.
[68] J. Deng, A. Dunaevsky, Delayed development of dendritic spines in Fxr2 knockout mouse, Open Neurosci. J. 3 (2009) 148–153.
[69] E.A. Nimchinsky, A.M. Oberlander, K. Svoboda, Abnormal development of dendritic spines in FMR1 knock-out mice, J. Neurosci. 21 (2001) 5139–5146.
[70] H. Kasai, M. Matsuzaki, J. Noguchi, N. Yasumatsu, H. Nakahara, Structure–stability–function relationships of dendritic spines, Trends Neurosci. 26 (2003) 360–368.
[71] M. Matsuzaki, G.C. Ellis-Davies, T. Nemoto, Y. Miyashita, M. Iino, H. Kasai, Dendritic spine geometry is critical for AMPA receptor expression in hippocampal CA1 pyramidal neurons, Nat. Neurosci. 4 (2001) 1086–1092.

[72] A.E. Purcell, O.H. Jeon, A.W. Zimmerman, M.E. Blue, J. Pevsner, Postmortem brain abnormalities of the glutamate neurotransmitter system in autism, Neurology 57 (2001) 1618–1628.
[73] J.K. Angleson, W.J. Betz, Monitoring secretion in real time: capacitance, amperometry and fluorescence compared, Trends Neurosci. 20 (1997) 281–287.
[74] C. Levenes, H. Daniel, P. Soubrie, F. Crepel, Cannabinoids decrease excitatory synaptic transmission and impair long-term depression in rat cerebellar Purkinje cells, J. Physiol. 510 (Pt 3) (1998) 867–879.
[75] B. Szabo, I. Wallmichrath, P. Mathonia, C. Pfreundtner, Cannabinoids inhibit excitatory neurotransmission in the substantia nigra pars reticulata, Neuroscience 97 (2000) 89–97.
[76] E. Neher, Vesicle pools and Ca2 + microdomains: new tools for understanding their roles in neurotransmitter release, Neuron 20 (1998) 389–399.
[77] D.I. Orellana, R.A. Quintanilla, C. Gonzalez-Billault, R.B. Maccioni, Role of the JAKs/STATs pathway in the intracellular calcium changes induced by interleukin-6 in hippocampal neurons, Neurotox. Res. 8 (2005) 295–304.
[78] M.P. Perriol, K. Dujardin, P. Derambure, A. Marcq, J.L. Bourriez, E. Laureau, F. Pasquier, L. Defebvre, A. Destee, Disturbance of sensory filtering in dementia with Lewy bodies: comparison with Parkinson's disease dementia and Alzheimer's disease, J. Neurol. Neurosurg. Psychiatry 76 (2005) 106–108.